FEMS Microbiology Ecology, 93, 2017, fiw224

doi: 10.1093/femsec/fiw224
Advance Access Publication Date: 27 October 2016
Research Article

RESEARCH ARTICLE

Optical properties of dissolved organic matter relate to different depth-specific patterns of archaeal and bacterial community structure in the North Atlantic Ocean

Elisa Guerrero-Feijóo[1,†], Mar Nieto-Cid[2], Eva Sintes[3], Vladimir Dobal-Amador[1,4], Víctor Hernando-Morales[5], Marta Álvarez[1], Vanessa Balagué[6] and Marta M. Varela[1,*]

[1]IEO, Instituto Español de Oceanografía, Centro Oceanográfico de A Coruña, Apdo. 130, 15080, A Coruña, Spain, [2]IIM-CSIC, Instituto de Investigacións Mariñas, 36208 Vigo, Spain, [3]Department of Limnology and Bio-Oceanography, University of Vienna, A-1090, Vienna, Austria, [4]Departamento de Bioquímica, Xenética e Inmunoloxía, Universidade de Vigo, 36200 Vigo, Spain, [5]Departamento de Ecoloxía e Bioloxía Animal, Universidade de Vigo, 36200 Vigo, Spain and [6]ICM-CSIC, Institut de Ciències del Mar, 08003, Barcelona, Spain

*Corresponding author: Instituto Español de Oceanografía (IEO), Centro Oceanográfico de A Coruña, Apdo. 130, 15080, A Coruña, España. Tel: +34 981205362; Fax: +34 981229077; E-mail: marta.varela@co.ieo.es
One sentence summary: Optical properties of the DOM shaping microbial communities in the North Atlantic.
Editor: Gary King
†Elisa Guerrero-Feijóo, http://orcid.org/0000-0002-9524-6059

ABSTRACT

Prokaryotic abundance, activity and community composition were studied in the euphotic, intermediate and deep waters off the Galician coast (NW Iberian margin) in relation to the optical characterization of dissolved organic matter (DOM). Microbial (archaeal and bacterial) community structure was vertically stratified. Among the Archaea, Euryarchaeota, especially Thermoplasmata, was dominant in the intermediate waters and decreased with depth, whereas marine Thaumarchaeota, especially Marine Group I, was the most abundant archaeal phylum in the deeper layers. The bacterial community was dominated by Proteobacteria through the whole water column. However, Cyanobacteria and Bacteroidetes occurrence was considerable in the upper layer and SAR202 was dominant in deep waters. Microbial composition and abundance were not shaped by the quantity of dissolved organic carbon, but instead they revealed a strong connection with the DOM quality. Archaeal communities were mainly related to the fluorescence of DOM (which indicates respiration of labile DOM and generation of refractory subproducts), while bacterial communities were mainly linked to the aromaticity/age of the DOM produced along the water column. Taken together, our results indicate that the microbial community composition is associated with the DOM composition of the water masses, suggesting that distinct microbial taxa have the potential to use and/or produce specific DOM compounds.

Keywords: pyrosequencing; diversity; DOM optical properties; marine microbes; CARD-FISH; T-RFLP; ARISA; deep sea; Atlantic waters

Received: 19 April 2016; **Accepted:** 25 October 2016

INTRODUCTION

Marine microbes are major components of plankton and play a significant role in the oceanic biogeochemical cycles. Prokaryotic abundance and activity decrease with depth by one and two orders of magnitude, respectively (Arístegui *et al.* 2009; Furhman, Cram and Needham 2015). Such a pattern is determined by the vertical variability of the physical and chemical features of the pelagic environment, which also contribute to the vertical stratification of microbial community composition (DeLong *et al.* 2006; Martín-Cuadrado *et al.* 2007; Agogué *et al.* 2011).

Sequencing (Sanger and 454 pyrosequencing) of the rRNA gene is a valuable tool to characterize the microbial community structure in the water column (Giovannoni *et al.* 1996; DeLong *et al.* 2006; Yokokawa *et al.* 2010; Agogué *et al.* 2011; Lekunberri *et al.* 2013). Based on these techniques, several recent investigations have shown a vertical stratification of the microbial populations in the deep waters of the Atlantic Ocean (Agogué *et al.* 2011; Lekunberri *et al.* 2013; Ferrera *et al.* 2015, Frank *et al.* 2016) and Pacific Ocean (Schmidt, DeLong and Prace 1991; DeLong *et al.* 2006). In addition, variations in relative abundance of Archaea and Bacteria among different water masses have also been well established by catalyzed reporter deposition fluorescence *in situ* hybridization (CARD-FISH) enumeration of specific phylogenetic groups. CARD-FISH studies revealed increasing relative abundance of archaeal cells with depth while Bacteria shows the opposite pattern (Karner, DeLong and Karl 2001; Teira *et al.* 2006; Varela, van Aken and Herndl *et al.* 2008a,b; Dobal-Amador *et al.* 2016). Similarly, the distribution of specific groups of Bacteria varies considerably with depth (Varela *et al.* 2008b; Lekunberri *et al.* 2013; Doval-Amador *et al.* 2016). However, variation of the microbial community's composition with depth is not only attributable to the most abundant taxa, but also to the less abundant phylotypes. Recent results from next generation sequencing of the 16S rRNA gene indicate the existence of microbial phylotypes specific to the deep water masses of the Atlantic Ocean (Agogué *et al.* 2011; Ferrera *et al.* 2015).

Temperature, hydrostatic pressure and salinity correlate with the variation in abundance, activity and diversity of microbial communities (Sjöstedt *et al.* 2014; Furhman *et al.* 2015; Doval-Amador *et al.* 2016). The amount and quality of organic matter in marine ecosystems is also recognized as a major factor that affects the metabolism, distribution and dynamics of prokaryotic communities (Cottrell and Kirchman 2000; Kirchman *et al.* 2004; Dobal-Amador *et al.* 2016). However, our knowledge on the sources of DOM in the intermediate and deep waters and the link between the composition and diversity of DOM and microbial communities, particularly Archaea, in the dark ocean is still limited.

The Galician coast (NW Spain) is a dynamic area characterized by seasonal upwelling pulses, which support the export offshore and sinking of organic matter. Hence this ecosystem represents an ideal study area to investigate how the composition and diversity of DOM might shape microbial communities. Results from a previous exploratory study in the same area indicated that the bacterial community structure assessed by automated rRNA intergenic spacer analysis (ARISA) fingerprinting was related not only to physico-chemical parameters but also to DOM quality (Dobal-Amador *et al.* 2016). The aim of the present study was to extend these previous results and investigate the role of DOM quality and quantity in shaping the archaeal community structure as compared with Bacteria, by using terminal restriction fragment length polymorphism (T-RFLP)/ARISA fingerprinting and sequencing of the bacterial and archaeal 16S rRNA gene, along a longitudinal section off the eastern North Atlantic. We hypothesized that vertical variation in the different indices of the DOM results in different depth-related patterns in archaeal community structure as compared with Bacteria. We used the distance-based multivariate analysis for a linear model (DistLM) and redundancy analysis (RDA) to identify the best set of optical properties of organic matter explaining the variations in the archaeal community structure and composition as compared with Bacteria in the euphotic, intermediate and bathypelagic waters of the eastern North Atlantic.

MATERIAL AND METHODS

Sampling

Sampling was conducted during the cruises BIO-PROF-1 (11–28 August 2011) and BIO-PROF-2 (11–20 September 2012), on board R/V Cornide de Saavedra from 43°N, 9°W to 43°N, 14°W off Cape Finisterre (NW Spain) (Fig. 1). Samples were collected with Niskin bottles mounted on a conductivity–temperature–depth (CTD) rosette sampler from different depths based on their temperature and salinity: euphotic zone (EZ, three samples, 5, 50 and 100 m depth); Eastern North Atlantic Central Water (ENACW, two samples, 250–300 and 500–900 m depth) – the layer of the oxygen minimum zone (OMZ; ∼900 m); Mediterranean Water (MW, one sample, 1000 m depth); Labrador Sea Water (LSW, one sample, 1800 m depth); Eastern North Atlantic Deep Water (ENADW, one sample, 2750 m depth) and Lower Deep Water (LDW, one sample, >4000 m depth). A total of 43 stations were sampled (22 and 21 stations for BIO-PROF-1 and BIO-PROF-2, respectively) to perform the physical and chemical analysis (Fig. 1). Seawater samples from six stations (5, 8, 11, 16, 108 and 111; Fig. 1) were collected for dissolved organic matter measurements, and four stations (11, 16, 108 and 111; Fig. 1) were additionally sampled for microbial analysis, including abundance, activity, structure and composition of the prokaryotic communities in both cruises.

Chemical analysis

Samples for the analysis of dissolved oxygen measurements were collected in Pyrex 'iodine titration' flasks with flared necks and ground glass stoppers, with a nominal volume of about 115 mL. Following Langdon (2010), the samples were measured by the Winkler potentiometric method. Nutrient salts (nitrate, nitrite, phosphate and silicate) were collected in rinsed polyethylene bottles and frozen at –20°C until further analysis by standard colorimetric methods on a segmented flow analyzer (Bran–Luebbe) following the procedures of Hansen and Koroleff (1999).

All DOM samples above 200 m were filtered under positive pressure using an acid-clean all-glass system and combusted (450°C, 4 h) GFF filters. Water samples for the analysis of dissolved organic carbon (DOC) were collected in combusted (450°C, 12 h) glass ampoules, and acidified with H_3PO_4 to pH <2. The ampoules were heat-sealed and DOC was determined with a Shimadzu TOC-CSV analyzer by high temperature Pt-catalytic oxidation (Álvarez-Salgado and Miller 1998). The intensity of the fluorescent DOM (FDOM) was measured on board within 2–3 h at two pair of fixed excitation/emission wavelengths: 320 nm/410 nm (FDOM-M), characteristic of marine 'refractory' humic-like substances; and 280 nm/350 nm (FDOM-T), characteristic of 'labile' protein-like materials, using a Perkin Elmer LS55 following Nieto-Cid, Alvarez-Salgado and Perez (2006). Samples were calibrated against quinine sulfate and results are given in quinine sulfate units (QSU). UV-visible absorption spectra

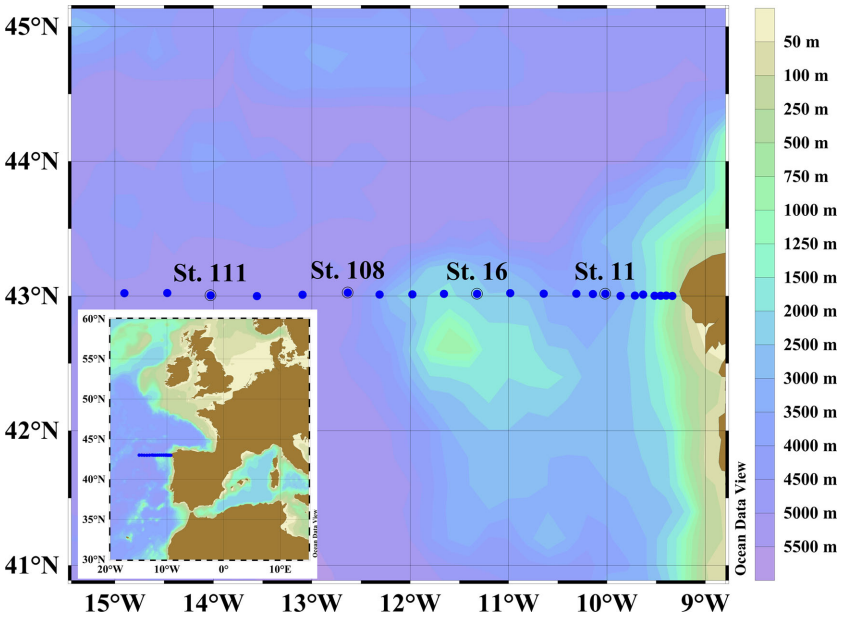

Figure 1. Map showing the stations along the Finisterre Section located in the NW Atlantic Ocean off the Galician coast. Dots represent the stations where the physico-chemical data were measured. The stations where the biological measurements were conducted are also indicated (St 11, St 16, St 108 and St 111).

of the chromophoric DOM were acquired on a Beckman Coulter DU800 spectrophotometer equipped with 10 cm quartz cuvettes also in a time frame of 2–3 h after collection. Spectral scans were recorded from 250 to 700 nm, using the sample average absorbance between 600 and 700 nm to correct for offsets (Green & Blough 1994). Absorption coefficients were calculated following Green & Blough (1994) at several wavelengths along the spectra aCDOM254 (absorption coefficient at 254 nm), aCDOM340 (absorption coefficient at 340 nm) and aCDOM365 (absorption coefficient at 365 nm). Differences between these indices lay on the nature of the colored DOM, as the intensification of the conjugation/aromaticity increases with the absorption wavelength (Stedmon & Nelson 2015). Thus, absorption coefficients at wavelength larger than 300 nm would only gather information for complex/aromatic molecules and would not be related to relatively simple compounds. In addition, the shape of the absorption spectra was explored by means of the spectral slopes between 275 and 295 nm (sCDOM275-295), calculated from the linear regression of log-transformed absorption spectra, and providing information on shifts in molecular mass and DOM aromaticity (Helms *et al.* 2008). In general terms, absorption coefficients are considered 'quantitative' variables, as they are a proxy of the concentration of colored DOM, while the slope of the spectra is assessed as a 'qualitative' variable, indicating changes in colored DOM composition (Stedmon and Nelson 2015).

Prokaryotic abundance

Following Gasol *et al.* (1999) samples for prokaryotic abundance (PA) were determined by flow cytometry. A volume of 1.8 mL per water sample was preserved with 1% paraformaldehyde (final concentration), shock-frozen in liquid N_2 for 10 min and stored at –80°C. Samples were thawed to room temperature and stained with Syto13 (Life Technologies) in the dark for 10 min. Subsequently, 1 μm fluorescent latex beads (approximately 1×10^5 mL^{-1}) (Molecular Probes, Invitrogen, Carlsbad, CA, USA) were added to all the samples as internal standard. The prokaryotes were counted using a FACSCalibur flow cytometer (Becton Dickinson, Franklin Lakes, NJ, USA) according to their signature in right angle light scatter and green fluorescence.

Leucine incorporation rates

Leucine incorporation (Leu incorp.) rates from the microbial communities from the euphotic and upper intermediate waters (up to 500 m) were measured by adding 5 nmol L^{-1} [^{3}H]leucine (final concentration, specific activity 160 Ci mmol L^{-1}, GE Healthcare, Little Chalfont, UK) to triplicate 1.2 mL samples. Duplicate trichloroacetic acid (TCA)-killed blanks (5% final concentration) were treated in the same way as the samples (Simon and Azam 1989). Samples and blanks were incubated in the dark and *in situ* temperature in temperature-controlled chambers for 2–6 h, depending on the expected activity. Incubations were terminated by adding TCA (5% final concentration) to the samples. Bacterial proteins were precipitated by two successive centrifugation steps (12350g, 10 min), including a washing step with 1 mL of 5% TCA following Kirchman, Knees and Hodson (1985) with slight modifications (Smith and Azam 1992).

Leu incorp. from the lower intermediate and deep waters (below 1000 m) was determined by adding 5 nmol L^{-1} [^{3}H]leucine (final concentration, specific activity 160 Ci mmol L^{-1}, GE Healthcare) to duplicate 40 mL samples and duplicate formaldehyde-killed blanks (2% final concentration) (Simon and Azam 1989). The incubation of samples and blanks was carried out in the dark and *in situ* temperature for 10–24 h, depending on the expected activity. The incubations were finished by adding formaldehyde (2% final concentration) to the samples. Samples and blanks were filtered onto 0.2 μm polycarbonate filters (25 mm filter diameter, Millipore). Afterwards, the filters were rinsed with 10 mL 5% ice-cold TCA and air-dried before liquid scintillation cocktail was added to the vials. After 18 h, the radioactivity was quantified in a scintillation counter (LBK Wallac). The disintegrations per minute (DPMs) of the blanks were

subtracted from the mean DPMs of the respective samples and the resulting DPMs converted into leucine incorporation rates. The cell-specific activity was estimated dividing Leu incorp. by PA.

DNA extraction of the prokaryotic community

A volume of 10–15 L of water was filtered through sterile Sterivex 0.22 μm pore size filters (Millipore, USA); 1.8 mL of lysis buffer (40 mM EDTA, 50 mM Tris–HCl, 0.75 M sucrose) was added to the filter cartridge and stored at –80°C. DNA extraction was performed by enzymatic lysis of the cells with lysozyme and proteinase K, followed by phenol–chloroform extraction. DNA was precipitated by the addition of isopropanol. The pellet was washed with 70% ethanol and resuspended in sterile TE buffer. DNA samples were quantified and quality checked (according to the A_{260}/A_{280} ratio) using a Nanodrop spectrophotometer (Thermo Scientific, USA).

T-RFLP and ARISA fingerprinting of archaeal and bacterial communities

Two different fingerprinting techniques, T-RFLP and ARISA, were performed to study archaeal and bacterial community structure, respectively. Both techniques can be used to quickly profile the structure of microbial communities. The internal transcribed spacer (ITS) region used for ARISA is more variable than the 16S rRNA used for T-RFLP. Slightly higher total numbers of bacterial operational taxonomic units (OTUs) have been obtained with ARISA as compared with T-RFLP (Yokokawa *et al.* 2010). Thus, ARISA has been suggested to be more effective than T-RFLP on the 16S rRNA for estimating diversity of prokaryotic assemblages (García-Martinez *et al.* 1999). However, several Archaea harbor very short or even lack intergenic transcribed spacer (Moreira, Rodríguez-Varela and López-García 2004, Leuko *et al.* 2008). Taking these previous findings into account, we used ARISA fingerprinting to assess the bacterial community structure and T-RFLP was performed to assess the archaeal community structure.

T-RFLP fingerprinting was carried out on a standard amount of DNA (2 μL) from each sample by using the primer set 27F-FAM (FAM-6′-AGA GTT TGA TCC TGG CTC AG-3′) and 958R-VIC (VIC-5′-YCC GGC GTT GAM TCC ATT T-3′; DeLong 1992). PCR conditions and chemicals were applied as described by Moeseneder *et al.* (2001). PCR product was purified and subsequently digested at 37°C overnight with the tetrameric restriction enzyme (HhaI). The restriction enzyme was heat inactivated and the digested DNA was precipitated. Fluorescently labelled fragments were separated and detected in an ABI Prism 310 capillary sequencer (Applied Biosystems). The internal size standard used were LIZ 1200 (20–1200 pb, Applied Biosystems). The output from the ABI Genescan software was analyzed with the FINGERPRINTING II software (Bio-Rad) to determine the peak height.

Automated rRNA intergenic spacer analysis (ARISA)-PCR was conducted on a standard amount of DNA (2 μL) from each sample. Bacterial ARISA was performed using ITSF, 5′-GTC GTA ACA AGG TAGGCC GTA-3′, and ITSReub, 5′-GCC AAG GCA TCC ACC 3′, primer sets (Thermo Scientific) as previously described (Cardinale *et al.* 2004). ARISA fingerprinting conditions have been previously reported (Dobal-Amador *et al.* 2016). ARISA fragments were separated using the ABI Prism 3730XL (Applied Biosystems) genetic analyzer applying the internal standard LIZ 1200 (20–1200 pb; Applied Biosystems). Obtained peaks with height value <20 fluorescence units were removed from the output peak matrix before statistical analyses. Each ARISA peak was defined as a different OTU.

Pyrosequencing of the archaeal and bacterial 16S rRNA gene

Pyrosequencing was performed for Archaea and Bacteria only at station 111 during the BIO-PROF 2 cruise. We analyzed seven samples, representative of the different water masses in this region. A subsample of the DNA extracted was used for pyrosequencing at the Research and Testing Laboratory (Lubbock, TX, USA: http://medicalbiofilm.org) using 454 GL FLX technology. The Bacteria-specific primers 28F (5′GAGTTTGATCNTGGCTCAG) and 519R (5′GTNTTACNGCGGCKGCTG) were used to generate amplicons from V1 to V3 regions of the bacterial 16S rRNA gene (~500 bp). Archaea-specific primers 341F (5′-GYGCASCAGKCGMGAAW-3′) and 958R (5′-GGACTACVSGGGTATCTAAT-3′) were used to amplify the region spanning the V3 to V5 regions (~600 bp). Subsequent analyses were performed using the Quantitative Insights Into Microbial Ecology (QIIME) pipeline (http://qiime.org) (Caporaso *et al.* 2010).

A quality check was performed to minimize low quality pyrotags, eliminating sequences with 50 bp sliding window Phred average below 25, ambiguous bases and sequences with length <100–125 bp after trimming. The remaining sequences were run into Denoiser to detect the pyrosequencing errors (Reeder and Knight 2010). The curated sequences were grouped into OTUs with a 97% similarity threshold. A representative sequence from each phylotype was chosen by selecting the most abundant sequence in each cluster. MOTHUR was used to remove chimeras by ChimeraSlayer (Schloss *et al.* 2009; Haas *et al.* 2011) based on the alignment file SILVA 108 (http://www.arb-silva.de). Blast Classifier (Wang *et al.* 2007) implemented in QIIME determined the identity of 16S rRNA phylotypes. OTUs assigned to chloroplast or mitochondria were removed from our analysis. In addition, the rarefraction curves were plotted to verify that the sequences obtained in each sample showed a tendency of plateauing for the most samples of Archaea (Supplementary Fig. S1a) and Bacteria (Supplementary Fig. S1b). Pyrotag sequences have been deposited in the National Center for Biotechnology Information (NCBI) Sequence Read Archive (SRA) under PRJNA317990 and PRJNA318014 bioproject numbers.

One OTU table was built for Archaea and another for Bacteria. Both tables were subsampled to ensure an equal number of sequences per sample (1436 and 3511sequences for Archaea and Bacteria, respectively).

CARD-FISH and FISH

CARD-FISH was used to quantify the abundance of the major of prokaryotic groups at four stations (11, 16, 108 and 111) following the method described by Pernthaler, Pernthaler and Amann (2002). Immediately after collecting the samples from the Niskin bottles, 20–80 mL of seawater was preserved with paraformaldehyde (2% final concentration) and stored at 4°C in the dark. About 12–18 h later, the samples were filtered onto 0.2 μm polycarbonate filters (Millipore GTTP, 25 mm filter diameter) supported by nitrocellulose filters (Millipore, HAWP, 0.45 μm), washed twice with 10 mL Milli-Q water, dried and stored in a microfuge vial at –20°C until further analysis. Filters were cut in sections and hybridized with horseradish peroxidase (HRP)-labelled oligonucleotide probes (Supplementary Table S1), followed by tyramide-Alexa488 signal amplification. Cells were counter-stained with a DAPI-mix [5.5 parts of Citifluor (Citifluor), 1 part of Vectashield (Vector Laboratories) and 0.5 parts of phosphate-buffered saline (PBS) with DAPI (final concentration

2 μg mL^{-1})]. Quantification of DAPI-stained cells and cells stained with the specific probes was carried out under a Nikon Eclipse 80i epifluorescence microscope equipped with Hg lamp and appropriate filter sets for DAPI, Cy3 and Alexa448. A minimum of 500 DAPI-stained cells were counted per sample.

Statistical analysis

All t-test analysis was performed using Sigmaplot 8.0. Hierarchical cluster analysis (CLUSTER) was carried out to explore similarities between samples, based on the Bray–Curtis similarity matrix obtained by T-RFLP and ARISA fingerprintings of archaeal and bacterial communities. Significant differences in microbial community composition between samples were investigated by permutational analysis of variance with PRIMER software (Primer-E v. 6; Anderson 2001). The differences in alpha diversity among water masses (by using the 454-pyrosequencing data) were tested statically using ANOSIM analysis of the PRIMER software.

A distance-based linear model (DistLM) analysis was used to study the relationship between the resemblance matrix of microbial community structure and DOM-related variables. Previously, all variables were tested for co-linearity (Spearman correlation matrix) and those with determination coefficients (R^2) higher than 0.95 were eliminated. The contribution of each variable was assessed, firstly using 'marginal test' to assess the statistical significance and percentage contribution of each variables taken separately. Secondly, a 'sequential test' was employed to evaluate the cumulative effect of each variable once the previous variable(s) had been accounted for. All variables were introduced in the model with the 'step wise' selection procedure of the DistLM model, using the 'Akaike' information criterion (AIC). Such a procedure allows us to find the best combination of variables that explain the variability from the microbial resemblance matrix. All statistical tests were performed with PRIMER6 and PERMANOVA+ (Anderson, Gorley and Clarke 2008). In addition, a redundancy analysis (RDA) was performed to examine the associations among DOMvariables and specific microbial groups obtained using 454-pyrosequencing with XLSTAT software.

RESULTS

Environmental parameters

The main water masses along a section off the Galician coast (Fig. 1) were identified according to their temperature and salinity signals (Prieto *et al.* 2013). The physical and chemical characteristics of these water masses are summarized in Table 1. No significant differences were detected for the physico-chemical variables between the two cruises (t-test, $P > 0.5$, $n = 555$ for temperature, salinity and oxygen; t-test, $P > 0.5$, $n = 371$ for nitrate, silicate and phosphate). The Lower Deep Water (LDW) was found below 4000 m depth. LDW is characterized by low temperature (2.5°C; Table 1), low salinity (34.4; Table 1), high dissolved oxygen (250 μmol kg^{-1}; Supplementary Fig. S2a and b), nitrate (20 μmol kg^{-1}; Supplementary Fig. S2c and d), phosphate (1.5 μmol kg^{-1}; Supplementary Fig. S2e and f) and silicate concentration (32.8–44.94 μmol kg^{-1}; Supplementary Fig. S2g and h). The Eastern North Atlantic Deep Water (ENADW) was identifiable by slightly higher temperature (2.5–3.5°C; Table 1) and higher oxygen concentration (Supplementary Fig. S2a and b; Prieto *et al.* 2013; Dobal-Amador *et al.* 2016). Two types of intermediate waters were found: the Labrador Sea Water (LSW; 1800–2000 m) showed a minimum of salinity (35.0–35.4; Table 1) and a relatively high oxygen concentration (197.5–262.8 μmol kg^{-1}; Supplementary Fig. S2a and b), and the Mediterranean Water (MW; 1000 m depth) was clearly identifiable by the highest salinity values (35.0–36.2; Prieto *et al.* 2013; Table 1) as compared with the other water masses. The Eastern North Atlantic Central Water (ENACW) was found between 250 and 900 m depth and the oxygen minimum zone (OMZ) was located east of the Galician bank at around 900 m depth characterized by the lowest oxygen concentrations (180–241 mol kg^{-1}; Supplementary Fig. S2a and b). The lowest concentrations of nitrate, phosphate and silicate (0.1–8.7, 0.1–0.7 and 0.2–4.4 μmol kg^{-1}, respectively) were found in the euphotic zone (EZ; 0–100 m depth).

Elemental and optical characterization of the DOM

The DOC concentration decreased from subsurface towards the deeper layers (Fig. 2a and b) with no significant differences between BIO-PROF-1 and BIO-PROF-2 cruises (t-test, $P = 0.19$, $n = 107$). The lowest DOC concentrations (42–44 μmol L^{-1}) were determined in the LDW. The fluorescence of protein-like substances of the DOM showed significant differences between the two cruises (t-test, $P < 0.01$, $n = 107$), being lower during BIO-PROF-1. FDOM-T also decreased with depth, from 1.84 QSU at the EZ and reaching values of about 0.30 QSU in LDW (Fig. 2c and d). By contrast, the fluorescence of marine humic-like substances increased from ~0.60 QSU in EZ to 1.00 in LDW (Fig. 2e and f) and did not exhibit significant differences between the two cruises (t-test, $P = 0.13$, $n = 107$). The absorption coefficient at 254 nm (aCDOM254) (Fig. 3a and b) ranged from 1.32 at EZ to 0.84 at LDW with no significant differences between the cruises (t-test, $P = 0.52$, $n = 107$). On the other hand, aCDOM340 and aCDOM365 (Fig. 3c–f) did not show any clear vertical trend, presenting average values of 0.13 and 0.09, respectively. However, significant differences were found between both cruises

Table 1. Physical and chemical characteristics of the main water masses sampled during the cruises BIO-PROF-1 and BIO-PROF-2 along the northwestern Iberian Peninsula (Cape Finisterre). ENACW-OMZ, Eastern North Atlantic Central Water – oxygen minimum zone; ENADW, Eastern North Atlantic Deep Water; EZ, euphotic zone; LDW, Lower Deep Water; LSW, Labrador Sea Water; MW, Mediterranean Water.

Water mass	Depth (m)	Temperature (°C)	Salinity	Oxygen (μmol kg^{-1})	Nitrate (μmol kg^{-1})	Silicate (μmol kg^{-1})	Phospate (μmol kg^{-1})
EZ	≤100	12.47–20.45	35.73–36.11	189.81–269.16	0.10–8.71	0.22–4.40	0.10–0.72
ENACW-OMZ	250–900	10.11–12.92	35.54–36.11	180.47–243.71	7.31–19.50	2.12–8.07	0.51–1.11
MW	1000	3.6–11.42	35.03–36.15	180.58–261.7	13.03–21.44	6.64–12.69	0.72–1.31
LSW	1800–2000	3.56–7.25	34.96–35.21	197.50–261.78	15.54–19.49	9.63–15.23	0.91–1.31
ENADW	2500–2900	2.51–3.50	34.92–35.04	235.13–255.94	14.63–22.96	10.59–35.12	1.02–1.49
LDW	≥4000	2.47–2.54	34.89–34.91	232.03–243.70	18.30–23.23	32.82–47.10	1.24–1.56

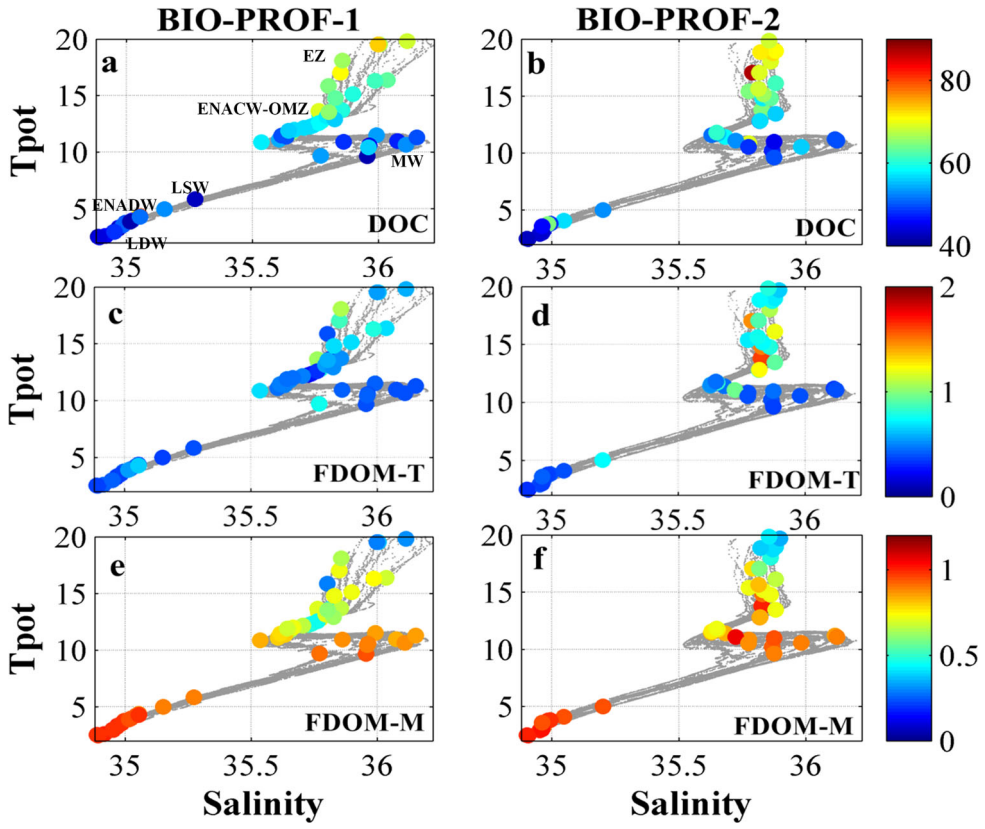

Figure 2. Potential temperature (T_{pot}, °C)–salinity diagrams every 2 dbars for BIO-PROF-1 (left) and BIO-PROF-2 (right), with superimposed values from discrete depths for (**a, b**) DOC in μmol kg^{-1}, (**c, d**) protein-like fluorescence (FDOM-T) and (**e, f**) humic-like fluorescence (FDOM-M).

(t-test, $P < 0.01$, $n = 107$), as both coefficients were higher in the shallower waters during BIO-PROF-2. The sCDOM275-295 decreased from 0.033 in the EZ to 0.027 in the LDW and significant differences were found between both cruises (t-test, $P < 0.01$, $n = 54$).

Prokaryotic abundance and leucine incorporation

The highest prokaryotic abundance (PA) occurred in the EZ ((2.33 ± 0.8) × 10^5 cells mL^{-1}; Fig. 4a and b), decreasing exponentially with depth at all stations during both BIO-PROF-1 and BIO-PROF-2 cruises. No significant differences among PA distribution in the two cruises were observed (t-test, $P = 0.67$, $n = 58$). The minimum values were found in the ENADW ((1.84 ± 0.94) × 10^4 cells mL^{-1}; Fig. 4b) during BIO-PROF-2 cruise. The rates of leucine incorporation (Leu incorp.) showed a similar vertical trend at both cruises, decreasing three orders of magnitude from the EZ (7.85 ± 5 fmol Leu L^{-1} day^{-1}; Fig. 4c and d) to the LDW ((6.68 ± 6.75) × 10^{-3} fmol Leu L^{-1} day^{-1}; Fig. 4c and d). Cell-specific activity decreased from the euphotic zone to the intermediate and deep waters; however, it varied between cruises (Fig. 4e and f). Maximum cell-specific activity was (1.46 ± 1.5) × 10^{-5} fmol Leu cell^{-1} day^{-1} in the EZ during the BIO-PROF-1 cruise (Fig. 4e). Generally, cell-specific activity was more variable in the intermediate and deep waters, particularly during the BIO-PROF-2 cruise, but always within one order of magnitude. In the intermediate and deep waters, the minimum cell-specific activity was (9.81 ± 6.98) × 10^{-6} fmol Leu cell^{-1} day^{-1} in the LDW during BIO-PROF-1, while the maximum was (1.13 ± 1.04) × 10^{-3} fmol Leu cell^{-1} day^{-1} in the EZ during BIO-PROF-2.

Microbial community structure determined by fingerprinting techniques

The T-RFLP pattern of the archaeal community revealed a total of 133 OTUs at the 16S rRNA gene level, ranging from 46 to 918 bp. The T-RFLP fingerprints of specific water masses showed 106 OTUs in the EZ, 49 OTUs in the ENACW-OMZ, 68 OTUs in the MW, 56 OTUs in the LSW, 67 OTUs in the ENADW and 26 OTUs in the LDW. Fourteen per cent of the 135 OTUs were present in all water masses; by contrast, 35% were unique to specific water masses. The archaeal community clustered according to different water masses (Supplementary Fig. S3a): (i) the first cluster corresponded to archaeal communities inhabiting the euphotic zone (labelled in blue, Supplementary Fig. S2a); (ii) the second set corresponded to archaeal communities in intermediate waters, ENACW-OMZ and MW (labelled in orange, Supplementary Fig. S3a); and (iii) the third cluster corresponded to the deep waters, represented by LSW, ENADW and LDW (labelled in green, Supplementary Fig. S3a).

On the other hand, the ARISA patterns of the bacterial community revealed in total 290 different bacterial taxa (OTUs) on the ITS region, ranging from 101 to 1017 bp. The ARISA profiles for the different water masses comprised 206 OTUs in the EZ, 172 OTUs in the ENACW-OMZ, 151 OTUs in the MW, 154 OTUs in the LSW, 169 OTUs in the ENADW and 124 OTUs in the LDW. Sixteen per cent of the 290 OTUs were present in all water masses; by contrast, 21% were unique to specific water masses. These specific OTUs led to a clear separation of bacterial communities according to three main groups of water masses: (i) one cluster comprised bacterial communities inhabiting in EZ (labeled in blue, Supplementary Fig. S3b); (ii) the second cluster

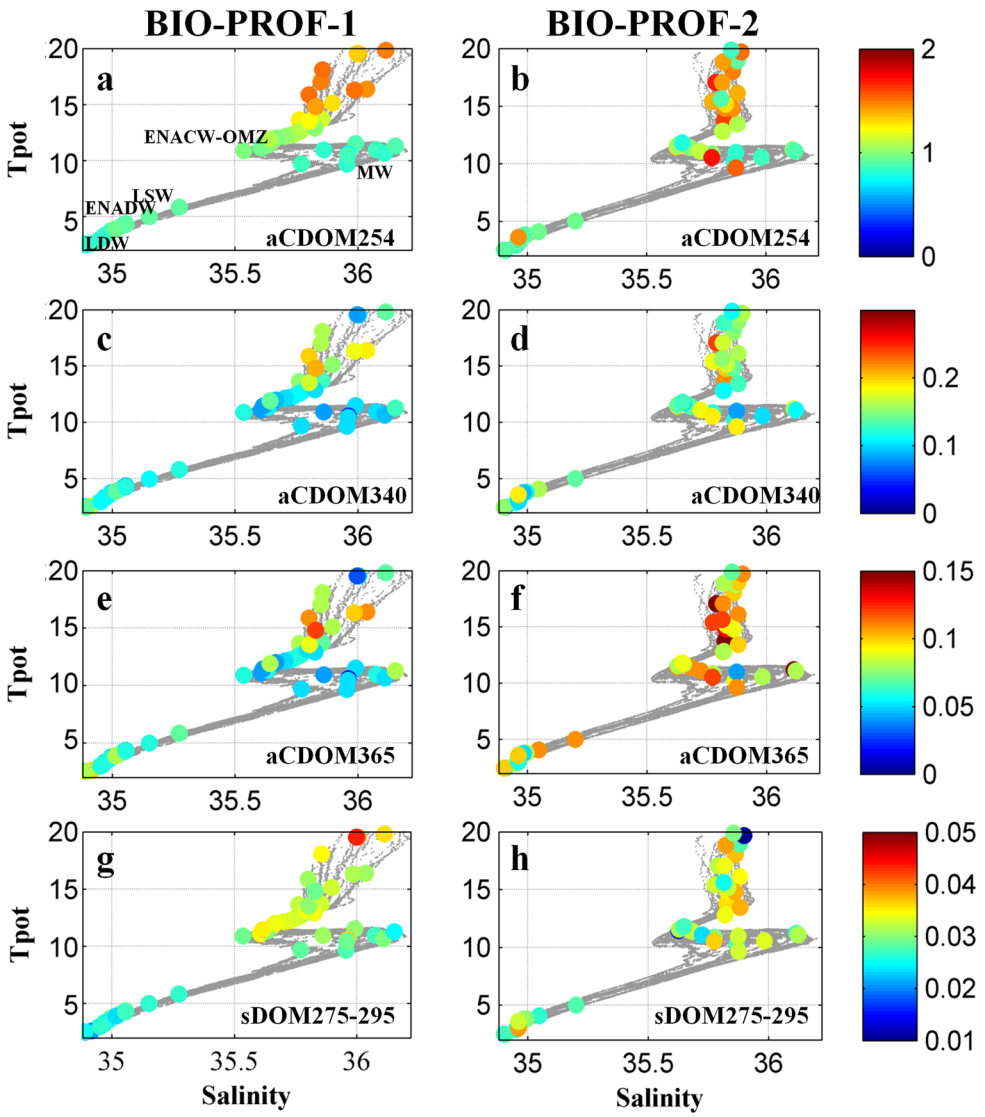

Figure 3. Potential temperature (T_{pot}, °C)–salinity diagrams every 2 dbars for BIO-PROF-1 (left) and BIO-PROF-2 (right), with superimposed values from discrete depths for (**a, b**) absorption coefficient at 254 nm, (**c, d**) absorption coefficient at 365 nm and (**e, f**) optical slope between 275 and 295 nm.

consisted of bacterial communities inhabiting the intermediate water masses, ENACW-OMZ and MW (labeled in orange, Supplementary Fig. S3b); (iii) and the third cluster comprised the bacterial communities from the deep waters, comprising LSW, ENADW and LDW (labeled in green, Supplementary Fig. S3b).

Microbial community composition assessed by 454-pyrosequencing

A total of 29 336 archaeal (on average 4191 sequences per sample, range 1436–8043) and 80 659 bacterial (on average 13 443 sequences per sample, range 3511–45 269) sequences were obtained by 454-pyrosequencing from 7 samples, after quality check and denoising of the raw sequences. The total number of OTUs for Archaea and Bacteria was 275 and 1309, respectively. The highest richness (Chao1 richness index) of Archaea occurred in ENACW-OMZ (141) decreasing towards the ENADW, which showed the minimum value (41; Supplementary Table S2). Subsequently, the richness increased again at LDW (51). Similarly, Bacteria also revealed a maximum of Chao1 index richness in the ENACW-OMZ (638) and decreased with depth reaching the minimum in the LDW (222; Supplementary Table S2).

The taxonomy of Archaea (Fig. 5a) and Bacteria (Fig. 5b) was studied at the order and family level. The archaeal community was composed of the phyla Euryarchaeota and Thaumarchaeota, contributing 17 and 83% to the total archaeal 16S rRNA gene sequences, respectively. Euryarchaeota was dominated by Thermoplasmata, mainly by Marine Group II (MGII) with an average relative abundance among all water masses of 14%, and relative abundances up to 40% in the ENACW-OMZ and LSW. Additionally, on average 3% of the sequences were identified as Marine Group III (MGIII). The most abundant order of Thaumarchaeota was Marine Group I (MGI 81%) with the maximum relative abundance located in the EZ and MW (Fig. 5a).

The bacterial community showed a larger number of different phyla compared with Archaea (Fig. 5b). Taking into account the whole Bacteria dataset, we found that most sequences belonged to the phyla Proteobacteria (80%). The most abundant classes of Proteobacteria were the Alphaproteobacteria (56%) with the highest abundance found in the EZ (82%). Delta- and

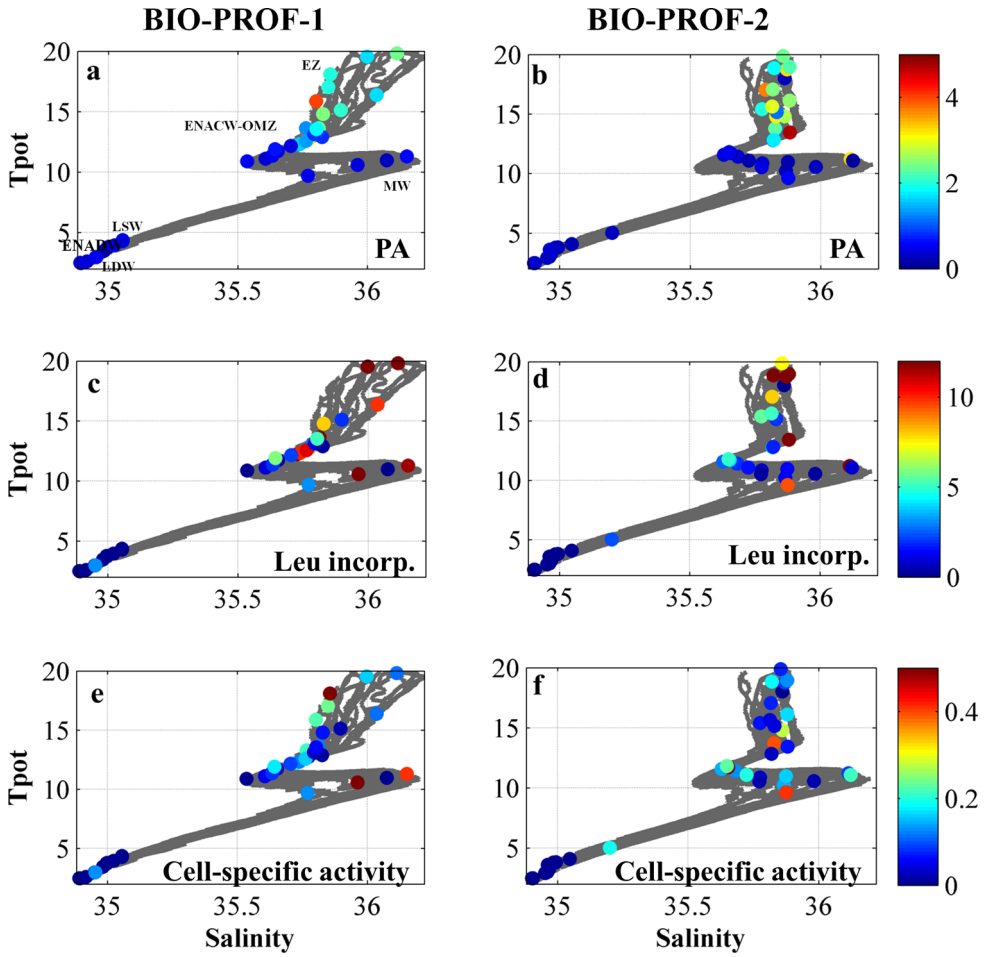

Figure 4. Potential temperature (T_{pot}, °C)–salinity diagrams every 2 dbars for BIO-PROF-1 (left) and BIO-PROF-2 (right), with superimposed values from discrete depths for (**a, b**) prokaryotic abundance (10^5 cells mL^{-1}), (**c, d**) leucine incorporation rate (pmol Leu L^{-1} h^{-1}) and (**e, f**) cell-specific activity (10^{-4} pmol Leu $cell^{-1}$ h^{-1}).

Gammaproteobacteria made up to 14 and 8% of total Bacteria, respectively. Deltaproteobacteria accounted for 24% of total Proteobacteria in the LSW, while Gammaproteobacteria showed the highest abundance located in the LDW (36% of total Proteobacteria). Interestingly, Vibrionaceae accounted for 3.5% of total bacterial sequences; however, 24.3% of Vibrionaceae sequences were found in the LDW. Cyanobacteria sequences, belonging to Prochlorococcus, were on average 6% of the total bacterial community, and showed the maximum relative abundance in the ENACW-OMZ. Additionally, SAR202 (4%) was the dominant group within the Chloroflexi class, with maximum relative abundance in the ENADW and LDW. Other less abundant groups were Bacteroidetes (3%), Actinobacteria (2%), Deferribacteres (1%) and Planctomycetes (1%). Despite the majority of the samples being dominated by Proteobacteria, differences between the different water masses were observed at lower phylogenetic levels. Flavobacteriaceae was present in the ENACW-OMZ (3%; Fig. 5b). Within Alphaproteobacteria, we found three members of SAR11 at the family level (SAR11 clade, SAR11 surface and SAR11 deep). SAR11 clade and SAR11 surface were more abundant in the EZ and ENACW-OMZ (Fig. 5b) as compared with SAR11 deep or SAR11 clade. However, SAR11 deep showed the highest relative abundance in the LSW (Fig. 5b). Rhodospirillaceae had higher relative abundance in the MW and in the LSW than Ricketssiales, which peaked in the ENADW and LDW (Fig. 5b). Nitrospinaceae, the second most abundant group of Deltaproteobacteria, was relatively more abundant in the EZ and MW (Fig. 5b) than in deep waters. Within Gammaproteobacteria, the most frequent phylotypes at family level were Colwellia, JL-ETNP-Y6 (Oceanospirilla), Oceanospirillaceae and Vibrionaceae. These phylotypes showed their maximum relative abundance in the LDW (Fig. 5b). The relative abundance of Mariprofundaceae (Zetaproteobacteria) ranged between 0.1 and 1% of total bacteria, with maximum values located in the MW and ENADW.

Bacterial and archaeal abundance assessed by CARD-FISH

The contribution of Bacteria to the total prokaryotic community decreased from the euphotic zone (~60%) to the deep waters (~45%) (Table 2). By contrast, the relative abundance of Thaumarchaeota (% of DAPI, Table 2) tended to increase with depth. The highest relative abundance was found in the oxygen minimum zone and deep waters; however, Thaumarchaeota never reached values higher than ~15%. The abundance of both Thaumarchaeota and Bacteria did not show significant differences between BIO-PROF-1 and BIO-PROF-2 (*t*-test, $P > 0.05$, $n = 22$).

DOM variables influencing the microbial communities

A marginal test was performed to explain the contribution of each DOM variable separately on the archaeal community

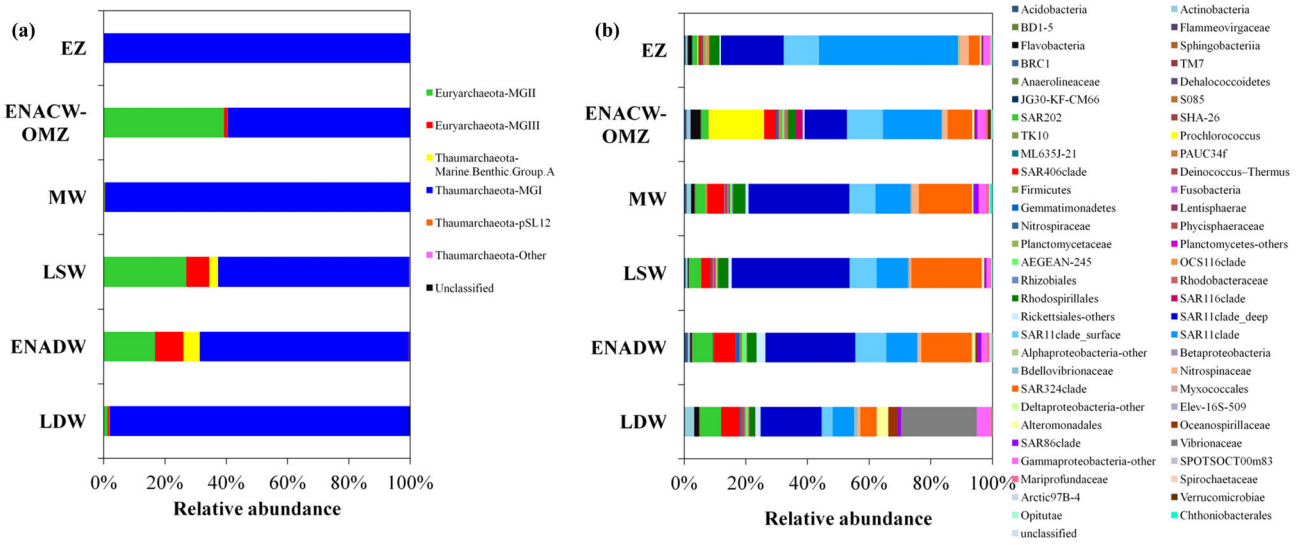

Figure 5. Taxonomic classification of (a) archaeal and (b) bacterial sequences retrieved from different water masses at the family level from 16S rRNA gene pyrosequencing. For water mass abbreviations see Table 1.

Table 2. Relative abundance of the major groups of prokaryotes, Thaumarchaeota and Bacteria (% of DAPI), in the different water masses off the Galician coast (Cape Finisterre). For water-mass abbreviations see Table 1.

Water masses	Bacteria	Thaumarchaeota
EZ	54.58 ± 15.08	5.34 ± 2.42
ENACW-OMZ	48.85 ± 5.18	9.52 ± 2.82
MW	43.70 ± 7.03	9.36 ± 3.48
LSW	41.78 ± 5.55	8.22 ± 2.18
ENADW	37.83 ± 5.11	12.98 ± 3.89
LDW	44.51 ± 2.17	14.09 ± 2.17

structure using T-RFLP fingerprinting and bacterial community structure using ARISA fingerprinting results. DOC, FDOM-T, FDOM-M, aCDOM254, sCDOM275-295 and depth were significantly related with the archaeal community composition (Supplementary Table S3). FDOM-M and FDOM-T were the main explanatory factors identified by DistLM of the archaeal community structure (Table 3) for the whole dataset ($n = 48$), explaining together 18% of the total variability. However, different depth layers showed different predictor variables. The main predictor factor for the variability in archaeal community structure in the EZ ($n = 11$) was aCDOM254, explaining 22.3% of the total variation. FDOM-T, aCDOM254, depth, sCDOM275-295, DOC and FDOM-M explained most of the variability in archaeal community structure in the intermediate waters (54.4%, $n = 19$). In the deep waters ($n = 18$), FDOM-M was the only significant variable, accounting for 11.7% of the variation in archaeal community structure (Table 3).

Similarly, the marginal test for bacterial communities revealed significant effects of DOC, FDOM-T, FDOM-M, sCDOM275-295 and depth (Supplementary Table S4). Considering the whole water column ($n = 63$), the DistLM sequential test showed that FDOM-M, depth, aCDOM365, aCDOM340, FDOM-T and sCDOM275-295 were related with the bacterial community composition, explaining 36% of the total variation (Table 4). However, depth was the only variable that significantly explained the variation in the bacterial community structure from the EZ (13.2%; $n = 18$). sCDOM275-295, depth and aCDOM340 accounted for 29.2%, 12.1% and 5.7% of the total variation in bacterial community structure from the intermediate waters ($n = 25$). The main predictor factors for the variability in bacterial

Table 3. Multivariate regression analysis (DistLM) of variables contributing to explaining the archaeal community structure with 'step-wise' selection procedure on the Akaike information criterion as selection criterion (sequential test). P, the significance level; %Var, percentage of variation explained by each variable; %Cumul, cumulative percentage variance. Statistically significant values are shown in bold (P value < 0.05).

Depth layer	Variable	Pseudo-F	P	%Var	%Cumul
Total	FDOM-Ms	7.1726	**0.001**	13.49	13.49
($n = 48$)	FDOM-T	2.7069	**0.014**	4.91	18.40
EZ ($n = 11$)	aCDOM254	2.585	**0.015**	22.31	22.31
Intermediate (ENACW-OMZ, MW) ($n = 19$)	FDOM-T	2.4385	**0.040**	12.55	12.55
	aCDOM254	2.3295	**0.042**	11.12	23.66
	Depth	2.3541	**0.024**	10.36	34.02
	sCDOM275-295	2.1236	**0.035**	8.69	42.71
	DOC	1.5705	0.131	6.18	48.88
	FDOM-M	1.4421	0.187	5.48	54.37
Deep (LSW, NEADW, LDW) ($n = 18$)	FDOM-M	2.1115	0.042	11.66	11.66

Table 4. Multivariate regression analysis (DistLM) of variables that contribute to explain the bacterial community structure with 'step-wise' selection procedure on the Akaike information criterion as selection criterion (sequential test). *P*, the significance level; %Var, percentage of variation explained by each variable; %Cumul, cumulative percentage variance. Statistically significant values are shown in bold (*P* value < 0.05).

Depth layer	Variable	Pseudo-F	*P*	%Var	%Cumul
Total ($n = 63$)	FDOM-M	10.541	**0.001**	14.73	14.73
	Depth	5.2119	**0.001**	6.81	21.55
	aCDOM365	3.7877	**0.001**	4.73	26.28
	aCDOM340	3.7000	**0.001**	4.42	30.70
	FDOM-T	2.3326	**0.016**	2.72	33.43
	sCDOM275-295	2.3070	**0.012**	2.63	36.06
EZ ($n = 18$)	Depth	2.4216	**0.016**	13.15	13.15
Intermediate (ENADW-OMZ, MW) ($n = 25$)	sCDOM275-295	4.7230	**0.002**	17.04	17.04
	Depth	3.7751	**0.001**	12.15	29.19
	aCDOM340	1.8321	0.090	5.68	34.87
Deep (LSW, NEADW, LDW) ($n = 20$)	Depth	2.5866	**0.017**	12.57	12.57
	sCDOM275-295	2.4778	**0.044**	11.12	23.69
	aCDOM365	1.8587	0.067	7.94	31.63

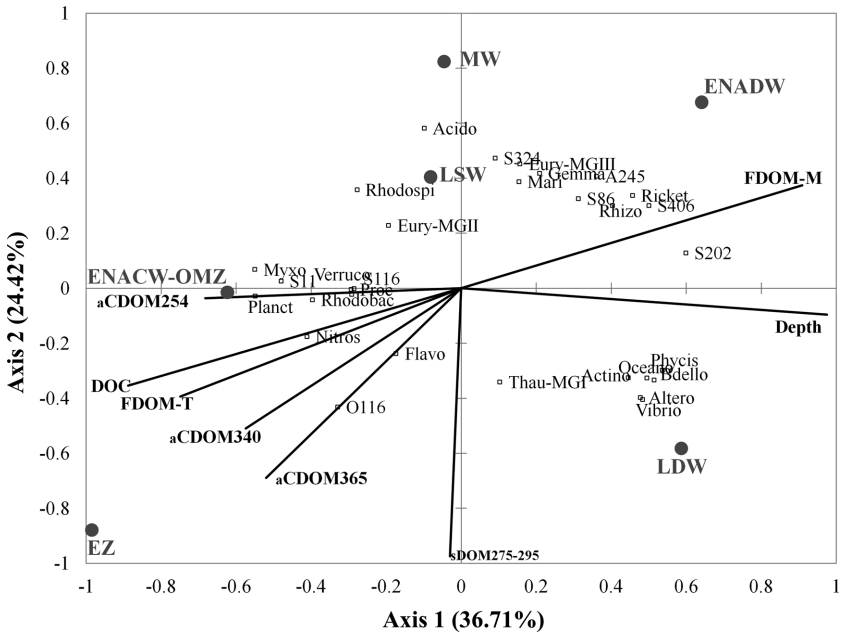

Figure 6. Redundancy analysis (RDA) of microbial groups obtained with 454-pyrosequencing and DOM variables. The filled circles represent the water masses sampled and the stars represent the microbial phylogenetic groups. The direction of the rows indicates the direction of increase in the variable and the length corresponds to DOM variables. For water mass abbreviations see Table 1. Acido, Acidobacteria; Actino, Actinobacteria; Flavo, Flavobacteria; Proc, Prochlorococcus; Gemma, Gemmatimonadetes; Phycis, Phycisphaeraceae; Planct, Planctomycetes; A245, AEGAN-245; Rhizo, Rhizobiales; Rhodobac, Rhodobacteraceae; Rhodospi, Rhodospirillales; Ricket, Rickettsiales; Bdello, Bdellovibrionaceae; Nitros, Nitrospinaceae; Myxo, Myxococcales; Altero, Alteromonadales; Oceano, Oceanopirillaceae; Vibrio, Vibrionaceae; Mari, Mariprofundaceae; Verru, Verrucomicrobia; Eury-MGII, Euryarchaeota-MGII; Eury-MGIII, Euryarchaeota-MGIII; Thau, Thaumarchaeota.

community from the deep waters ($n = 20$) were the aCDOM365, depth and sCDOM275-295, with 7.9%, 11.1% and 12.6%, respectively (Table 4).

Redundancy analysis (RDA) was performed to examine how DOM variables were associated to specific microbial 454-pyrosequencing phylotypes (Fig. 6). Microbial phylotypes in the different water masses were associated to different DOM variables. Axes 1 and 2 were interpreted as (i) depth/DOM quantity and (ii) DOM quality, respectively.

The FDOM-M showed positive correlation with both axes. Depth presented a positive correlation with axis 1 and negative correlation with axis 2. sCDOM275-295, aCDOM365, aCDOM340, aCDOM354 and FDOM-T displayed a negative correlation with axis 1 and positive correlation with axis 2. In addition, Euryarchaeota-MGIII, which had its highest relative abundance in ENADW, was significantly associated to FDOM-M. Furthermore, sCDOM275-295 was connected to Thaumarchaeota-MGI and also to the bacterial groups Acidobacteria and SAR324 clade. Flavobacteria and OCS116 clade were related to aCDOM365. RDA also suggests a strong link between aCDOM254 and bacterial members inhabiting ENACW-OMZ, i.e. SAR11 clade, Rhodobacterales, SAR116 clade and Verrucomicrobia.

Additionally, the DOC concentrations were correlated with the relative abundance of Nitrospirillaceae. By contrast, the increasing relative abundance of SAR202 clade, SAR406 clade, SAR286 clade, Rickettsiales and Rhizobiales with depth was related to FDOM-M.

DISCUSSION

Archaeal and Bacterial communities inhabiting the euphotic, intermediate and deep waters have been described for the first time off the Galician coast. The microbial abundance, activity and community composition showed clear vertical trends consistent with the vertical stratification of environmental and optical characteristics of DOM. As expected, most of the DOM variables (DOC, FDOM-T and aCDOM254) presented higher concentrations at the surface and decreased with depth, whereas FDOM-M increases with depth, as described previously (Carlson and Hansell 2015; Stedmon and Nelson 2015). Globally, all the DOM values were consistent with previous measurements in this region (Lønborg and Álvarez-Salgado 2014). Correspondingly, the highest abundance and leucine incorporation of the prokaryotic communities was found in the euphotic zone, characterized by the highest temperature, oxygen and organic matter bioavailability that facilitate the growth of microbes. On the other hand, the abundance and activity decrease with depth by two and three orders of magnitude, respectively, and environmental conditions may only allow the growth of specific microbes associated to dark waters.

Vertical distribution of specific archaeal and bacterial phylotypes

Vertical microbial distribution patterns suggest habitat partitioning, where Bacteria are dominant at the surface waters and Archaea are more abundant in OMZ and deeper waters, as previously reported for other regions of the North Atlantic Ocean (Herndl *et al.* 2005; Teira *et al.* 2006; Varela *et al.* 2008b; Agogué *et al.* 2011).

Thaumarchaeota dominated over Euryarchaeota and exhibited a patchy vertical distribution. The high abundance of Thaumarchaeota-MGI found in the EZ and ENADW have also been observed in previous studies (Herndl *et al.* 2005; Teira *et al.* 2006; Varela *et al.* 2008b). Ferrera *et al.* (2015) found all Euryarchaeota related to the class Thermoplasmata in the northeastern Atlantic Ocean in agreement with our results off the Galician coast. The Euryarchaeota-MGII vertical distribution, with maximum relative abundance in the OMZ, indicates an adaptation of members of this group to low oxygen concentrations. The highest abundance of Thaumarchaeota in this area is found in layers with lower oxygen concentrations as compared with surface and deep waters, in agreement with previous studies in ocean ecosystems (Francis *et al.* 2005; Lam *et al.* 2007). These decreased oxygen layers are suitable for redox processes such as ammonia oxidization (Zehr and Ward 2002; Könneke, DeLong and Karl 2005; Sintes *et al.* 2013) and, consequently, the organisms inhabiting them can potentially exhibit autotrophic metabolism (Guerrero-Feijoo *et al.* 2015). However, Thaumarchaeota also showed high relative abundance in the euphotic zone and the deeper layers linked to the highest DOC concentration, suggesting mixotrophic metabolism and different substrate preferences for different Thaumarchaeota ecotypes (Sintes *et al.* 2016; Smith *et al.* 2016).

Our results support that members of the SAR11 clade of Alphaproteobacteria are the most abundant and ubiquitous bacterial organisms in the ocean, indicating high competition for available resources, particularly at the ocean surface (Giovannoni and Rappé 2000; Morris *et al.* 2002; DeLong *et al.* 2006; Dobal-Amador *et al.* 2016). By contrast, the Gammaproteobacteria were the dominant group in the deeper waters, particularly in the LDW, in accordance with current knowledge of bacterial communities from marine ecosystems (Lopez-Garcia *et al.* 2001; Sogin *et al.* 2006; Lauro and Bartlett 2008). Alteromonas identified by 16S rRNA gene 454 sequences showed a patchy distribution as compared with CARD-FISH counts from the same cruise which, showed a decreasing relative abundance with depth (Doval-Amador *et al.* 2016). Both 454-pyrosequencing of this study and CARD-FISH counts (Doval-Amador *et al.* 2016) showed a clear increasing trend of SAR324 clade with depth (maximum relative abundance was located in the LSW). The enrichment of this group could reflect an important role of chemoautotrophic metabolism in the deep water masses, since previous studies based on single cell genomic analyses have shown that members of the SAR324 clade contain sulfur oxidizing genes in the intermediate and deep waters and are capable of inorganic carbon fixation (Swan, Martinez-Garcia and Preston 2011; Sheik, Jain and Dick 2014).

SAR202 clade has been described as a bacterial phylotype in the deep North Atlantic waters (Varela *et al.* 2008b) and an r-strategist, which can rapidly exploit nutrient patches in the dark ocean (Varela *et al.* 2008b). Another prominent group in deep waters off the Galician coast was SAR406 clade, in agreement with previous reports (Gordon and Giovannoni 1996; Gallagher *et al.* 2004; Pham *et al.* 2008; Galand *et al.* 2010). SAR406 members contain inorganic sulfur metabolic pathways (Yamamoto and Takai 2011), suggesting a possible role of these organisms as sulfate reducers. Bacteroidetes is more abundant in surface than deep waters (Chauhan, Cherrier and Williams 2009), in agreement with their ability to use high molecular mass DOM biopolymers (Kirchman 2001).

Although a correlation between the results obtained by the CARD-FISH analysis (Doval-Amador *et al.* 2016) and the 16S rRNA gene amplicon 454-pyrosequencing could not be performed as these different techniques target different 16S gene regions, we found a good correspondence between the vertical distributions of the specific groups of Bacteria by both methodologies. The contribution of SAR324 and SAR406 to the bacterial community as determined by CARD-FISH and pyrosequencing was close to 1:1 (data not shown), indicating that both techniques retrieved this cluster with similar efficiency. By contrast, the relative abundance of SAR11 was higher in the pyrosequencing dataset than with CARD-FISH (data not shown, *t*-test, $P < 0.05$). Alteromonas and SAR202 contributed disproportionately more to bacterial abundance using CARD-FISH than using pyrosequencing (data not shown, *t*-test, $P < 0.05$). These different patterns could be explained either by the different number of samples analyzed with the two methodologies or as being due to the PCR bias associated with the pyrosequencing approach as compared with CARD-FISH, where the probes target directly the 16S rRNA.

Importance of DOM-related variables influencing the microbial community structure and composition

Microbial community composition correlates with a variety of abiotic parameters (such as temperature and salinity) of the water masses (Yokokawa *et al.* 2010; Agogué *et al.* 2011; Sjöstedt *et al.* 2014; Dobal-Amador *et al.* 2016). Moreover, microbial community composition varies according to DOM composition

(Kirchman *et al.* 2004). Several studies have found that the microbial production of recalcitrant DOM (mostly humic substances) as a subproduct of the remineralization processes adds complexity to this relationship (Nieto-Cid, Alvarez-Salgado and Perez 2006; Jiao *et al.* 2010). Standard physico-chemical variables were the main factor explaining the variability of the bacterial community's vertical distribution in the deep waters of the Galician coast (Dobal-Amador *et al.* 2016). However, in this previous study it was also indicated that some optical DOM characteristics further explain the variability in the bacterial community structure through the water column (Dobal-Amador *et al.* 2016). Nevertheless, the DOM composition and the link between microbial communities and the DOM acting as substrate or subproduct of bacterial and archaeal metabolism in the deep ocean remain enigmatic. Both labile and refractory compounds, represented by FDOM-T and FDOM-M, respectively, related differently to the microbial communities off the Galician coast. Whereas the archaeal communities from the intermediate layers are linked to more labile molecules (protein-like material), which could be preferentially respired by these organisms, the archaeal communities of the deep waters are related to more refractory compounds. The strong positive correlation among FDOM-M and the relative abundance of Archaea, particularly Euryarchaeota-MGII, support the concept of a microbial carbon pump (Jiao *et al.* 2010), as these deep-ocean microbial communities are more connected to the refractory DOM (humic-like compounds) generated by themselves as subproducts of their respiratory metabolism.

Variations in bacterial community structure of the samples from the EZ are associated with depth, which is probably related to temperature and other physical parameters (Yokokawa *et al.* 2010, Sjöstedt *et al.* 2014), as well as chlorophyll *a* and DOM availability (Walsh *et al.* 2015). sCDOM275-295 was the main explanatory DOM-related variable for bacterial community structure in the intermediate and deep waters, suggesting a tight coupling between the bacteria and the aromaticity and molecular mass of the DOM (Helms *et al.* 2008). This finding would indicate that the molecular mass of the DOM, very likely associated to DOM ageing in the water masses (Helms *et al.* 2008), is linked to the changes in the bacterial community structure within the dark ocean. The strong relationship of Acidobacteria and SAR324 clade, typical deep-sea groups, with sCDOM275-295 suggests a higher contribution of these organisms to transform DOM into older, bigger and more aromatic compounds. Furthermore, the relationship of bacterial communities from intermediate waters with aCDOM340 (mainly Nitrospirae) and the relationship of the bacterial communities inhabiting the deeper layers with aCDOM365 (Mariprofundaceae and Gemmatimonadetes) suggest that the deep water bacterial communities metabolize DOM with a higher degree of aromaticity (more refractory) than the bacterial communities of the intermediate waters (absorption wavelength of 365 nm *versus* 340 nm; Stedmon & Nelson 2015). The relationships between DOM variables and the distribution patterns of Flavobacteria, Myxococcales, SAR11 clade, SAR86 clade, SAR116 clade, SAR202 clade, SAR324 clade, SAR406 clade, Rhodobacteraceae, Rickettsiales, Planctomycetes and Verrucomicrobia support the notion of a heterotrophic (or mixotrophic) lifestyle of these groups. Flavobacteria (Bacteroidetes) and SAR86 (Gammaproteobacteria) have been reported before as important players in DOM cycling, especially for the high molecular mass fraction of DOM (Kirchman 2002; Nikard, Cottrell and Kirchman 2014). Nevertheless, several bacterial groups, such as SAR202 clade (Chloroflexi), SAR406 clade (Deferribacteres), Rickettsiales (Alphaproteobacteria) and Rhizobiales (Alphaproteobacteria), showed also a strong correlation with FDOM-M indicative of their potential to generate refractory compounds of DOM (humic-like compounds), as subproducts of the remineralization processes.

Our data suggest that both archaeal and bacterial communities are coupled to compositional changes in the DOM pool. The increasing/decreasing patterns of FDOM-M and FDOM-T with depth are the main variables related to the vertical stratification of microbial communities; however, the absorption coefficients at 254, 340 and 365 nm are also affected by the stratification of microbial communities in the eastern North Atlantic Ocean. Some phylotypes, such as SAR202 and SAR406, might be able to relate to both labile and refractory DOM, while others, such as Thaumarchaeota-MGI, display preferential relations with aromatic compounds in the deep waters.

SUPPLEMENTARY DATA

Supplementary data are available at *FEMSEC* online.

ACKNOWLEDGEMENTS

We thank the captain and the crew of R/V Coornide de Saavedra for their support during the BIO-PROF-1 and BIO-PROF-2 cruises. We thank F. Eiroa for assistance with onboard and flow cytomety measurements, C. Carballo for help with the inorganic nutrient analysis. X. A. Álvarez-Salgado, M. J. Pazó and J. Pampín for support with the chemical characterization, E. Teira and G. J. Herndl for support with the fingerprinting analysis and J. M. Gasol for support with the pyrosequencing bioinformatic analysis. High-Performance computing analyses were run at the Marine Bioinformatics Service of the Institut de Ciències del Mar (ICM-CSIC) in Barcelona. Funding for the sampling and analysis was provided by the projects 'Biodiversidade Funcional do Microplancton nas profundidades mariñas de Galicia' (BIO-PROF, Ref. 10MMA604024PR, 2010–2013, Xunta de Galicia) and 'Fuentes de Materia Orgánica y Diversidad Funcional del Microplancton en las aguas profundas del Atlántico Norte' (MODUPLAN, Ref. CTM2011-24008-MAR, 2012–2015, Plan Nacional I+D+I) to MMV. MNC was funded by the CSIC Program 'Junta para la Ampliación de Estudios' co-financed by the ESF (reference JAE DOC 040) and the project FERMIO (MINECO, CTM2014-57334-JIN). EG-F was supported by the BIO-PROF and MODUPLAN projects. VH-M was supported by the MICINN program 'Formación de Personal Investigador' (FPI), Ref. grant BES-2009-028186. ES was supported by the Austrian Science Fund (FWF) project P27696-B22. This work is in partial fulfillment of the requirements for a PhD degree from the Universidade de A Coruña by EG-F.

Conflict of interest. None declared.

REFERENCES

Agogué H, Lamy D, Neal PR *et al.* Water mass-specificity of bacterial communities in the North Atlantic revealed by massively parallel sequencing. *Mol Ecol* 2011;**20**:258–78.

Álvarez-Salgado XA, Miller AEJ. Simultaneous determination of dissolved organic carbon and total dissolved nitrogen in seawater by high temperature catalytic oxidation: conditions for precise shipboard measurements. *Mar Chem* 1998;**62**:325–33.

Anderson MJ. A new method for non-parametric multivariate analysis of variance. *Austral Ecol* 2001;**26**:32–46.

Anderson MJ, Gorley RN, Clarke KR. *PERMANOVA+ for PRIMER: Guide to Software and Statistical Methods* 2008. Plymouth, UK: PRIMER-E.

Arístegui J, Gasol JM, Duarte CM *et al.* Microbial oceanography of the dark ocean's pelagic realm. *Limnol Oceanogr* 2009;**54**: 1501–29.

Caporaso JG, Kuczynski J, Stombaugh J *et al.* QIIME allows analysis of high-throughput community sequencing data. *Nat Methods* 2010;**7**: 335–6.

Cardinale M, Brusetti L, Quatrini P *et al.* Comparison of different primer sets for use in automated ribosomal intergenic spacer analysis of complex bacterial communities. *Appl Environ Microbiol* 2004;**70**:6147–56.

Carlson CA, Hansell DA. DOM sources, sinks, reactivity, and budgets. In: Hansell DA, Carlson CA (eds). *Biogeochemistry of Marine Dissolved Organic Matter*, 2nd edn. Academic Press/Elsevier, 2015, 65–126.

Chauhan A, Cherrier J, Williams HN. Impact of sideways and bottom-up control factors on bacterial community succession over a tidal cycle. *Proc Natl Acad Sci U S A* 2009;**106**: 4301–6.

Cottrell MT, Kirchman DL. Community composition of marine bacterioplankton determinate by 16S rRNA gene clone libraries and fluorescence in situ hybridization. *Am Soc Microbiol* 2000;**66**:5116–22.

DeLong EF. Archaea in coastal marine environments. *Proc Natl Acad Sci U S A* 1992;**89**:5685–9.

DeLong EF, Preston CM, Mincer T *et al.* Community genomics among stratified microbial assemblages in the ocean's interior. *Science* 2006;**311**:496–503.

Dobal-Amador V, Nieto-Cid M, Guerrero-Feijóo E *et al.* Vertical patterns of bacterial abundance, activity and community composition in the dark waters of the Galician coast (NW Spain). *Deep Sea Res Part 1 Oceanogr Res Pap* 2016;**114**:1–11.

Ferrera I, Arístegui J, Gonzalez JM *et al.* Transcient changes in bacterioplankton communities induced by the submarine volcanic eruption of El Hierro (Canary Islands). *PLoS One* 2015;**10**:e0118136.

Francis CA, Roberts KJ, Beman JM *et al.* Ubiquity and diversity of ammonia-oxidizing archaea in water columns and sediments of the ocean. *Proc Natl Acad Sci U S A* 2005;**102**: 14683–8.

Frank AH, Garcia JA, Herndl GJ *et al.* Connectivity between surface and deep waters determines prokaryotic diversity in the North Atlantic Deep Water. *Environ Microbiol* 2016;**18**:2052–63.

Furhman JA, Cram JA, Needham DM. Marine microbial community dynamics and their ecological interpretation. *Nat Rev Microbiol* 2015;**13**:133–46.

Galand PE, Lovejoy C, Amilton AK *et al.* Archaeal diversity and gene for ammonia oxidation are coupled to ocean circulation. *Environ Microb* 2010;**11**:971–80.

Gallagher JM, Carton MW, Eardly DF *et al.* Spatio-temporal variability and diversity of water column prokaryotic communities in the eastern North Atlantic. *FEMS Microbiol Ecol* 2004;**47**:249–62.

García-Martinez J, Acinas SG, Anton AI *et al.* Use of the 16S–23S ribosomal genes spacer region in studies of prokaryotic diversity. *J Microbiol Methods* 1999;**36**:55–64.

Gasol JM, Zweifel U, Peters F *et al.* Significance of size and nucleic acid content heterogeneity as mesured by flow cytometry in natural planktonic bacteria. *Appl Environ Microbiol* 1999;**65**:104475–83.

Giovannoni S, Rappé M. Evolution, diversity, and molecular ecology of marine prokaryotes. In: Kirchman DL (ed.). *Microbial Ecology of the Oceans*, 1st edn. New York: John Wiley and Sons, Inc., 2000, 47–84.

Giovannoni SJ, Rappe MS, Vergin KL *et al.* 16S rRNA genes reveal stratified open ocean bacterioplankton populations related to the green non-sulfur bacteria. *Pro Natl Acad Sci U S A* 1996;**93**:7979–84.

Gordon DA, Giovannoni SJ. Detection of stratified microbial populations related to Chlorobium and Fibrobacter species in the Atlantic and Pacific Oceans. *Appl Environ Microbiol* 1996;**4**:1171–7.

Green SA, Blough NV. Optical absorption and fluorescence properties of chromophoric dissolved organic matter in natural waters, *Limnol Oceangr* 1994;**29**:1903–16.

Guerrero-Feijóo E, Nieto-Cid M, Sintes E *et al.* Bacterial activity and community composition response to the size-reactivity of disolved organic matter. In: Bertílsson S, Székely A (eds). *Second EMBO Conference on Aquatic Microbial Ecology (SAME-14)*. Abstract Program Book, p. 38. Uppsala, Sweden, 2015.

Haas BJ, Gevers D, Earl AM *et al.* Chimeric 16S rRNA sequence for mation and detection in Sanger and 454-pyrosequenced PCR amplicons. *Genome Res* 2011;**21**:494–504.

Hansen HP, Koroleff F. Determination of nutrients. In: Grasshoff K, Kremling K, Ehrhardt M (ed.). *Methods of Seawater Analysis*, 3rd edn. Weinheim: Wiley-VCH. 1999, 159–228.

Helms JR, Stubbins A, Ritchie JD *et al.* Absorption spectral slopes and slope ratios as indicators of molecular weight, source and photobleaching of chromophoric dissolved organic matter. *Limnol Oceanogr* 2008;**51**:2170–80.

Herndl GJ, Reinthaler T, Teira E *et al.* Contribution of Archaea to total prokaryotic production in the deep Atlantic Ocean. *Appl Environ Microbiol* 2005;**71**:2303–9.

Jiao N, Herndl GJ, Hansell DA *et al.* Microbial production of recalcitrant dissolved organic matter: long-term carbon storage in the global ocean. *Nat Rev Microbiol* 2010;**8**:593–9.

Karner MB, DeLong EF, Karl DM. Archaeal dominance in the mesopelagic of the Pacific Ocean. *Nature* 2001;**409**:507–10.

Kirchman DL. Measuring bacterial biomass production and growth rates from leucine incorporation in natural aquatic environments. In: Paul JH (ed.). *Methods in Microbiology*. San Diego: Academic Press, 2001, 227–37.

Kirchman DL. The ecology of Cytophaga-Flavobacteria in aquatic environments. *FEMS Microbiol Ecol* 2002;**39**:91–100.

Kirchman DL, Dittel AI, Findlay *et al.* Changes in bacterial activity and community structure in response to organic matter in the Hudson River, New York. *Aquat Microb Ecol* 2004;**34**: 243–57.

Kirchman DL, Knees E, Hodson R. Leucine incorporation and its potential as measure of protein synthesis by bacteria in natural aquatic system. *Appl Environ Microbiol* 1985;**49**: 599–607.

Könneke MB, DeLong EF, Karl DM. Isolation of an autotrophic ammonia-oxidizing marine archaeon. *Nature* 2005;**437**: 543–6.

Lam P, Jensen MM, Lavik G *et al.* Linking crenarchaeal and bacterial nitrification to anammox in the Black Sea. *Proc Natl Acad Sci U S A* 2007;**104**:7104–9.

Langdon C. Determination of dissolved oxygen in seawater by winkler titration using the amperometric technique. In: Hood EM, Sabine CL, Sloyan BM (eds). *GO-SHIP Repeat Hydrography Manual: A Collection of Expert Reports and Guidelines*, IOCCP Report No. 14, ICPO Publication Series No. 134. 2010. Available at: http://www.go-ship.org/HydroMan.html.

Lauro FM, Bartlett DH. Prokaryotic lifestyles in deep sea habitats. *Extremohiles* 2008;**12**:15–25.

Lekunberri I, Sintes E, De Corte D *et al*. Spatial patterns of bacterial and archaeal communities along the Romanche Fracture Zone (tropical Atlantic). *FEMS Microbiol Ecol* 2013;**85**:537–52.

Leuko S, Goh F, Ibáñez-Peral R *et al*. Lysis efficiency of standard DNA extraction methods for Halococcus spp. in an organic rich environment. *Extremophiles* 2008;**12**:301–8.

Lønborg C, Álvarez-Salgado XA. Tracing dissolved organic matter cycling in the eastern boundary of the temperate North Atlantic using absorption and fluorescence spectroscopy. *Deep Sea Res Part I* 2014;**85**:35–46.

Lopez-Garcia P, Lopez-Lopez A, Moreira D *et al*. Diversity of free-living prokaryotes from a deep-sea site at the Antarctic Polar Front. *FEMS Microbiol Ecol* 2001;**36**:193–202.

Martín-Cuadrado AB, López-García P, Alba JC *et al*. Metagenomics of the deep Mediterranean, a warm bathypelagic habitat. *PloS One* 2007;**2**:e914.

Moeseneder MM, Winter C, Arrieta JM *et al*. Terminal-restriction fragment length polymorphism (T-RFLP) screening of a marine archaeal clone library to determine the different phylotypes. *J Microbiol Methods* 2001;**44**:159–72.

Moreira D, Rodríguez-Varela F, López-García P. Analysis of a genome fragment of a deep-sea uncultivated Group II euryarchaeote containing 16S rDNA, a spectinomycin-like operon and several energy metabolism genes. *Environ Microbial* 2004;**6**:959–69.

Morris RM, Rappé MS, Connon SA *et al*. SAR11 clade dominates ocean surface bacterioplankton communities. *Nature* 2002;**420**:806–10.

Nieto-Cid M, Alvarez-Salgado XA, Perez FF. Microbial and photochemical reactivity of fluorescent dissolved organic matter in a coastal upwelling system. *Limnol Oceanogr* 2006;**51**:1391–400.

Nikard MP, Cottrell MT, Kirchman DL. Uptake of dissolved organic carbon by gammaproteobacterial subgroups in coastal waters of the West Antarctic Peninsula. *Appl Environ Microbiol* 2014;**80**:3362–8.

Pernthaler A, Pernthaler J, Amann R. Fluorescence in situ hybridization and catalyzed reported deposition for the identification of marine bacteria. *Appl Environ Microbiol* 2002;**68**:3094–101.

Pham VD, Konstantinidis KT, Palden T *et al*. Phylogenetic analyses of ribosomal DNA-containing bacterioplankton genome fragments from a 4000 m vertical profile in the North Pacific Subtropical Gyre. *Environ Microbiol* 2008;**10**:2313–30.

Prieto E, González-Pola C, Lavín S *et al*. Seasonality of intermédiate waters hydrography west of the Iberian Peninsula from an 8 year semiannual time series of an oceanographic section. *Ocean Sci* 2013;**9**:411–29.

Reeder J, Knight R. Rapidly denoising pyrosequencing amplicon reads by exploiting rank-abundance distributions. *Nat Methods* 2010;**7**:668–9.

Schloss PD, Westcott SL, Ryabin T *et al*. Introducing MOTHUR: Open-source, platform-independent, community-supported software for describing and comparing microbial communities. *Appl Environ Microbiol* 2009;**75**:7537–41.

Schmidt TM, DeLong EF, Prace NR. Analysis of a marine picoplankton community by 16S rRNA gene cloning and sequencing. *J Bacteriol* 1991;**173**:4371–8.

Sheik CS, Jain S, Dick GJ. Metabolic flexibility of enigmatic SAR324 revealed through metagenomics and metatranscriptomics. *Environ Microbiol* 2014;**16**:304–17.

Simon M, Azam F. Protein content and protein synthesis rates of planktonic marine bacteria. *Mar Ecol Progr Ser* 1989;**51**:201–13.

Sintes E, Bergauer K, De Corte D *et al*. Archaeal amoA gene diversity points to distintic biogeography of ammonia-oxidizing Crenarchaeota in the ocean. *Environ Microbiol* 2013;**15**:1647–58.

Sintes E, De Corte D, Haberleitner E *et al*. Geographic distribution of archaeal ammonia oxidizing ecotypes in the Atlantic Ocean. *Front Microbiol* 2016;**7**:77.

Sjöstedt J, Martiny JBH, Munk P *et al*. Abundance of broad bacterial taxa in the Sargasso Sea explained by environmental conditions but not water mass. *App Environ Microbiol* 2014;**80**:2786–94.

Smith DC, Azam F. A simple, economical method for measuring bacterial protein synthesis rates in seawater using 3H-leucine. *Mar Microb Food Webs* 1992;**6**:107–14.

Smith JM, Damashek J, Chavez FP *et al*. Factors influencing nitrification rates and the abundance and transcriptional activity of ammonia-oxidizing microorganisms in the dark northeast Pacific Ocean. *Limnol Oceanogr* 2016;**61**:596–60.

Sogin ML, Morrison HG, Huber JA *et al*. Microbial diversity in the deep sea and the underexploresd 'rare biosphere'. *Proc Natl Acad Sci U S A* 2006;**103**:12115–20.

Stedmon CA, Nelson NB. The optical properties of DOM in the ocean. In: Hansell DA, Carlson CA (eds). *Biogeochemistry of Marine Dissolved Organic Matter*, 2nd edn. Academic Press/Elsevier. 2015, 481–508.

Swan BK, Martinez-Garcia M, Preston CM. Potential for chemolithoautotrophy among ubiquitous bacteria lineages in the dark ocean. *Science* 2011;**333**:1296–300.

Teira E, van Aken H, Veth C *et al*. Archaeal uptake of enantiomeric amino acids in the meso- and bathypelagic waters of the North Atlantic. *Limnol Oceanogr* 2006;**54**:60–9.

Varela M, van Aken H, Herndl GJ. Abundance and activity of Cloroflexi-type SAR202 bacterioplankton in the meso- and bathypelagic waters of the (sub)tropical Atlantic. *Environ Microbiol* 2008a;**10**:1903–11.

Varela M, van Aken H, Sintes E *et al*. Latitudinal trends of Crenarchaeota and Bacteria in the meso- and bathypelagic waters of the Eastern North Atlantic. *Environ Microbiol* 2008b;**10**:110–24.

Walsh E, Smith D, Sogin M *et al*. Bacterial and archaeal biogeography of the deep chlorophyll maximum in the South Pacific Gyre. *Aquat Microb Ecol* 2015;**75**:1–13.

Wang Q, Garrity GM, Tiedje JM *et al*. Naieve Bayesian classifier for rapid assignment of rRNA sequences into the new bacterial taxonomy. *Appl Env Microbiol* 2007;**73**:5261–7.

Yamamoto M, Takai K. Sulfur metabolisms in epsilon- and gamma-Proteobacteria in deep-sea hydrothermal fields. *Front Microbiol* 2011;**2**:1–8.

Yokokawa T, DeCorte D, Sintes E *et al*. Spatial patterns of bacterial abundance, activity and community composition in relation to wáter masses in the eastern Mediterrean Sea. *Aquat Microbiol Ecol* 2010;**59**:185–95.

Zehr JP, Ward BB. Nitrogen cycling in the ocean: new perspectives on processes and paradigms. *Appl Environ Microbiol* 2002;**68**:1015–24.